Atmospheric Environment 99 (2014) 392–402

Contents lists available at ScienceDirect

Atmospheric Environment

journal homepage: www.elsevier.com/locate/atmosenv

SO_2 measurements at a high altitude site in the central Himalayas: Role of regional transport

Manish Naja [a], Chinmay Mallik [b,*], Tapaswini Sarangi [a], Varun Sheel [b], Shyam Lal [b]

[a] Aryabhatta Research Institute of Observational Sciences, Nainital, India
[b] Space and Atmospheric Sciences Division, Physical Research Laboratory, Ahmedabad, India

HIGHLIGHTS

- SO_2 over a pristine high altitude site in South Asia reported for the first time.
- Unlike many other sites in India, SO_2 levels over Nainital are lowest during winter.
- Diurnal variation shows daytime elevations throughout the year.
- Transport and PBL dynamics play crucial roles towards SO_2 levels over Nainital.

ARTICLE INFO

Article history:
Received 7 June 2014
Received in revised form
12 August 2014
Accepted 13 August 2014
Available online 14 August 2014

Keywords:
Sulfur dioxide
Boundary layer
Transport
NO_y
Free troposphere

ABSTRACT

Continuous measurements of a climatically important acidic gas, SO_2, were made over Nainital (29.37°N, 79.45°E; 1958 m amsl), a regionally representative site in the central Himalayas, for the first time during 2009–2011. Unlike many other sites, the SO_2 levels over Nainital are higher during pre-monsoon (345 pptv) compared to winter (71 pptv). High values during pre-monsoon are attributed to the transport of air masses from regions viz. Indo-Gangetic Plain (IGP), northern India and north-East Pakistan, which are dotted with numerous industries and power plants, where coal burning occurs. Transport from the polluted regions is evinced from good correlations of SO_2 with wind speed, NO_y and UV aerosol index during these periods. Daytime elevations in SO_2 levels, influenced by 'valley winds' and boundary layer evolution, is a persistent feature at Nainital. SO_2 levels are very much lower during monsoon compared to pre-monsoon, due to oxidation losses and wet scavenging. Despite this, SO_2/NO_y slopes are high (>0.4) both during pre-monsoon and monsoon, indicating impacts of point sources. The SO_2 levels during winter are lower as the measurement site is cut off from the plains due to boundary layer dynamics. Further, the SO_2 levels during winter nights are the lowest (lesser than 50 pptv) and resemble free tropospheric conditions.

1. Introduction

Sulfur dioxide (SO_2) is a primary criteria pollutant with potentially adverse health effects and concomitant deleterious impacts on the flora and fauna. SO_2 plays a pivotal role in the global sulfur cycle. It is a precursor of sulfate aerosols which exert a direct radiative forcing (RF) of -0.40 ± 0.20 W m^{-2} (Forster et al., 2007). One-half to two-thirds of this RF is attributable to anthropogenic sulfur (mainly SO_2). SO_2 may be transported several hundred kilometers (Mallik et al., 2013a) by virtue of an average tropospheric lifetime of ~1.8 days resulting from combined effects of gas-phase oxidation and dry deposition (Faloona, 2009). Despite global reductions in SO_2 emissions, a 70% growth is estimated over India during 1996–2010 (Lu et al., 2011). Most (91%) of these emissions are attributed to power-plants and industries (emitting 5236 and 2784 Gg SO_2 respectively in 2010). After power plants (constituting 46% SO_2 emissions in India), emissions from different industries is the second largest (36%) source of SO_2 (Garg et al., 2001). Almost a quarter of these industrial emissions come from steel sector, 14% from fertilizer plants, 10% from cement manufacturing and 7% from refineries. The SO_2 columnar burden over India has also shown an 83% increase, as detected from the Ozone Monitoring Instrument (OMI) observations (Lu et al., 2013). Further, modeling studies show high SO_2 over parts of the Indo Gangetic plain (IGP) but have not been corroborated by observations (Adhikary et al., 2007).

* Corresponding author. Present address: Max Planck Institute for Chemistry, Hahn-Meitner Weg 1, Mainz 55128, Germany.
E-mail addresses: chinmay.mallik@mpic.de, chinmay@prl.res.in (C. Mallik).

http://dx.doi.org/10.1016/j.atmosenv.2014.08.031
1352-2310/

Moreover, the seasonality in SO_2 levels and its conversion into sulfate is still an intriguing aspect, mainly over the Indian region due to lack of experimental data.

The IGP has been the focus of wide scientific deliberations due to occurrence of higher levels of trace gases and aerosols in this region, which are mainly due to larger anthropogenic, including agricultural, activities here. The IGP (area of about 0.7 million km^2) houses nearly a billion of the human population (about 1/7 of the global), making it one of the most populated and polluted river basins in the world. Despite being rich in fertile land and agricultural production, the fluvial landform has now been dotted with numerous industries including iron and steel, cement, chemicals etc. Rapid urbanization, changes in the land use pattern, emissions from the industries and power plants along with anthropogenic emissions from burning of fossil fuels and traditional bio-fuels by the population living here, has led to very high levels of pollutants viz. alkenes (Lal et al., 2012), ammonia (Clarisse et al., 2009), carbon monoxide (Kar et al., 2008), sulfur dioxide (Adhikary et al., 2007) etc. Even in case of secondary pollutants, high tropospheric ozone residual has been found along these plains throughout the year (Fishman et al., 2003).

The large emissions along the plains have implications to regional and global pollution, as deep convection during the summer–monsoon can efficiently lift the pollution to the upper troposphere, wherein it can then be transported to larger regions of the globe (Lawrence and Lelieveld, 2010; Baker et al., 2012). Further, high aerosol loading over the Ganga basin has been reported on the basis of ground-based observations (Dey and Tripathi, 2008) and satellite measurements (Ramanathan and Ramana, 2005). The shortwave atmospheric heating due to aerosols over the IGP is calculated to be greater than 0.4 K/day with a peak heating during pre-monsoon (>0.6 K/day) due to lower single scattering albedo and higher surface albedo (Ramachandran and Kedia, 2012). Positive trends in tropospheric temperatures have also been observed over urban regions in the IGP (Mallik and Lal, 2011) and have also been linked to IGP emissions (Gautam et al., 2009).

Due to a plethora of widely scattered emission sources, it is very difficult to find a representative site for characterizing the IGP emissions along the plains. This is because a representative site should be remotely located and sparsely inhabited to minimize in-situ emissions. In this perspective, observations from high-altitude stations assume special significance as measurements at these places can provide a "far-field picture", away from potential sources and provide a sort of background against which the urban impacts can be compared (Pant et al., 2006). Measurements of ozone at Nainital (29.37°N, 79.45°E; 1958 m amsl) suggest that it is an excellent regional representative site for gauging and characterizing the IGP emissions (Kumar et al., 2010b). Absence of daytime photochemical build-up in ozone (typical of urban or rural sites), established that local emissions of precursors were not significant to affect the ozone chemistry at the site. Being a high altitude site and away from any major anthropogenic activities, Nainital is a better site for conducting trace gas measurements. This has been validated from measurements of ozone (O_3) precursors viz. carbon monoxide (CO) and nitrogen oxides (NO_y) over Nainital (Sarangi et al., 2014). Trace gas measurements made over this region are expected to provide the information about background levels of these gases for the entire region.

Measurements of atmospheric constituents made over Nainital can provide opportunities to analyze various plumes e.g. aerosol measurements over this region were used to validate a volcanic plume (originating more than 5000 km away in Ethiopia) with SO_2 content in November, 2008 (Mallik et al., 2013a). Apart from sporadic transport plumes, measurements from this site can also be used to identify the contributions from downward transport, understand free tropospheric conditions as well as influence of regional pollution and biomass burning. In the present paper, we report levels and variability of SO_2 over Nainital using data from continuous, in-situ measurements over a period of three years during 2009–2011. These measurements have been made with a view to understand the levels and seasonality of SO_2 over the region and decipher emission characteristics of the pervading air masses.

2. Methodology

2.1. The observation site and general wind regimes

Observations are made at ARIES, Nainital (29.37°N, 79.45°E, 1958 m amsl), a high altitude site in the Central Himalayas (Fig. 1). The population of Nainital is less than 0.5 million and the region itself is devoid of large-scale industries. The nearest megacity, Delhi, is about 225 km away to the southwest. Sharply peaking mountains are located to the north and east of the observation site while mountains, with altitudes less than 1000 m in the south and west, separate the site from the IGP. In general, air masses at this site do not arrive from the northeastern sector in any season because of high mountains in that direction. The site is influenced by westerly winds during winter (December, January and February) and south-westerlies during monsoon (June–August). During pre-monsoon (spring, March–May), air masses are mostly north-westerly and transport pollutants from the northern Indian region and IGP to the observation site. Late spring (May) and early autumn (September) are the change over periods and winds mostly circulate over the Indian subcontinent. Throughout the year, except during pre-monsoon, about 10–15% of air masses influencing the observation site are from higher heights (>4000 m). During pre-monsoon, horizontal advection of air masses occurs at about 2 km amsl (Kumar et al., 2010b). Overall, the wind-direction being pre-dominantly north-westerly, potentially transport the north-

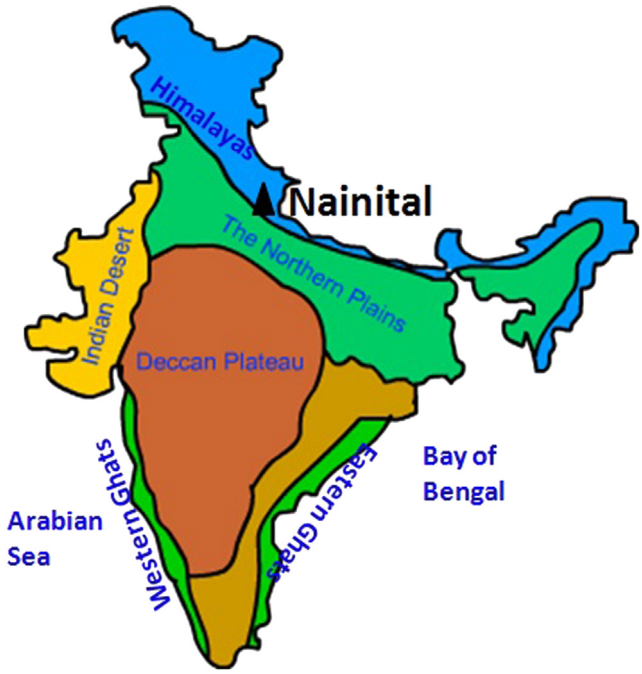

Fig. 1. The measurement site, ARIES (1958 m amsl), Nainital (black triangle) is located in the central Himalayas. Other major geographic sub-divisions of India are also shown in the map.

western IGP emissions to the study site. More than 50% of air masses originate in the 270–360° sector during January–June and about 40% during post-monsoon (September–November). However, during July–September, wind direction varies between northwesterly and south-easterly, with more than 35% air masses coming from the 90–180° and 270–360° sectors each, bringing emissions from the IGP to the site.

2.2. Experimental details

Continuous in-situ measurements of surface SO_2 were made over Nainital during January 2009–September 2011, using an online trace level gas analyzer from Thermo Scientific (43i-TLE). It is based on UV fluorescence (US EPA Equivalent Method – EQSA-0486-060) and achieves detection limit of 50 pptv with a 300 s averaging time. The linearity is 1% in the 0–1000 ppbv range and precision is about 1%. The ambient air is drawn from about 5 m above ground level through 5 m long PTFE (Biela et al., 2003) tubing (5 mm ID) into a Peltier unit (to remove moisture). The residence volume in this tube is about 0.1 L and assuming an average suction of 2 L/minute from all installed analyzers, the maximum residence time is 3 s. The air then enters the analyzer through a 5 μ PTFE filter (to remove dust) at 0.5 L/minute and passes through a hydrocarbon kicker within the instrument. The kicker removes hydrocarbons that fluoresce in the SO_2 region (Mohn and Emmenegger, 2001). The SO_2 molecules in the fluorescent chamber of the analyzer are then excited by pulsating UV light, generated through a narrow band-pass filter allowing only light wavelengths of 190–230 nm to pass into the chamber. A band pass filter centered around 350 nm is used to collect the fluorescence, which is measured by a PMT. Zero tests are made on a daily basis using in-situ generated zero air (by passing through a heatless air drier and silica gel, followed by scrubbing sequentially by Purafil, Puracoal and Charcoal). Further, the scrubbed air is then passed through a commercial zero air generator (Thermo Model 1160) where it is further scrubbed by passing it through a layer of activated charcoal (Hanke et al., 2003). Periodic span calibration is done using a dynamic gas calibrator (Thermo – 146i) and a gas mixture from Intergas (International Gases & Chemicals), UK (concentration: 471 ppbv in N_2, traceable to National Physical Laboratory, UK).

2.3. Auxiliary data sources

Measurements of meteorological parameters (solar radiation, air temperature, pressure, relative humidity, wind speed, wind direction and rainfall) were made using an automatic weather station (Campbell Scientific Inc., Canada and Astra Scientific, India). Fire data has been obtained from Moderate Resolution Imaging Spectroradiometer (MODIS) instrument aboard the Terra and Aqua satellites (http://modis-fire.umd.edu/AF_getdata.html). The Terra (Aqua) overpass time is around 1030 (1330) local solar time at the equator in its descending (ascending) mode and 2230 (0130) in nighttime. The planetary boundary layer heights (PBL, m) are obtained from MAAC reanalysis (http://data-portal.ecmwf.int/data/d/macc_reanalysis/). These boundary-layer heights are determined by lifting an air parcel from the surface layer up to the level where a critical bulk Richardson number is reached. The method is robust for both stable as well as unstable situations. The PBL data is obtained for the 1.125° × 1.125° grid centered at 29.25°N and 79.87°E for 0, 6, 12 and 18 GMT (0530, 1130, 1730 and 2330 IST respectively). The Indian standard time (IST) is 5 h and 30 min ahead of GMT. Columnar SO_2 amount for planetary boundary layer, free troposphere (DU) and UV aerosol index (Version3, Level 2; 0.25° × 0.25°), averaged over 22–23°N and 88–89°E, were obtained from the Ozone Monitoring Instrument (OMI) using the Giovanni interface. The OMI pass has a local equator crossing time of 1330 LT in the ascending node, hence supposedly represents daytime values. The PBL SO_2 columns are produced using the 'Band Residual Difference' algorithm (Krotkov et al., 2006), while TRM SO_2 (middle troposphere) are produced with the 'Linear Fit' algorithm (Yang et al., 2007). The UV Aerosol Index (AI) is a measure of the departure of the spectral dependence of the upwelling UV radiance of the actual atmosphere relative to that of a pure molecular atmosphere as given by accurate radiative transfer calculations. In general, non-zero AI values are produced solely by geophysical effects, and are mostly accounted by atmospheric aerosols.

2.4. MOZART model simulations

The Model for Ozone and Related chemical Tracers (MOZART) is a 3-D global chemical transport model of atmospheric composition designed to simulate both chemical and transport processes in the troposphere. Here we have used MOZART (ver 4.0) that deals with detailed anthropogenic hydrocarbon chemistry, improved scheme for determination of albedo, inclusion of tropospheric aerosols and online calculations of photolysis rates, dry deposition, H_2O concentration and biogenic emissions (Horowitz et al., 2003; Sheel et al., 2010). MOZART-4 simulates comprehensive tropospheric chemistry with 85 gas phase species, 12 bulk aerosol species, 39 photolysis and 157 gas-phase reactions (Emmons et al., 2010). The model simulation is done at a resolution of 2.8° × 2.8° (equivalent to T42) translating to 128 longitude and 64 latitude grid points; with 28 sigma pressure levels from the surface to ~2 mb using the NCEP's Global Forecast System (GFS) meteorological fields. The emission inventories for major anthropogenic sources, i.e. FF combustion and biofuel burning used in the present simulations are taken from the POET (Precursors of Ozone and their Effect on the Troposphere, an European Union project) for year 2000 (Olivier et al., 2003). The 1° × 1° POET inventory includes fire (monthly), natural emissions (monthly) and anthropogenic emissions (annual). These anthropogenic emissions have been updated over Asia for year 2006 using REAS (Regional Emission inventory in Asia version 1.1) inventory developed by Ohara et al. (2007) for a 0.5° × 0.5° grid. The monthly averaged BB emissions for the given year of simulation are taken from the Global Fire Emission Database, version 2 (GFED-v2). For SO_2, anthropogenic emissions are from the EDGAR-FT2000 database. Monthly average biomass burning emissions for each year for SO_2 are determined by scaling the GFED CO_2 emissions by the emission factors of Andreae and Merlet (2001) using the vegetation classification provided with GFED. SO_2 emissions from continuously outgassing volcanoes are from the GEIA-v1 inventory.

3. Results and discussion

3.1. Diurnal variations in surface SO_2

The seasonal average diurnal variations in surface SO_2 over Nainital is shown in Fig. 2. Average diurnal amplitude is maximum during pre-monsoon (MAM, 190 pptv) and minimum during monsoon (JJA, 26 pptv). The amplitudes during winter (DJF) and post-monsoon (SON) are found to be 61 and 37 pptv respectively. The diurnal amplitude is maximum during April (nearly 300 pptv), followed by March (209 pptv; early pre-monsoon) and February (136 pptv, late winter). Daytime PBL is highest during pre-monsoon period (about 2250 m and 1900 m at 1130 h and 1730 h IST). This facilitates transport processes, which are further augmented by high wind speeds (>2 m s^{-1}). Further, the amplitude of wind speed is highest during pre-monsoon (increases from 2 ms^{-1} at 0930 IST

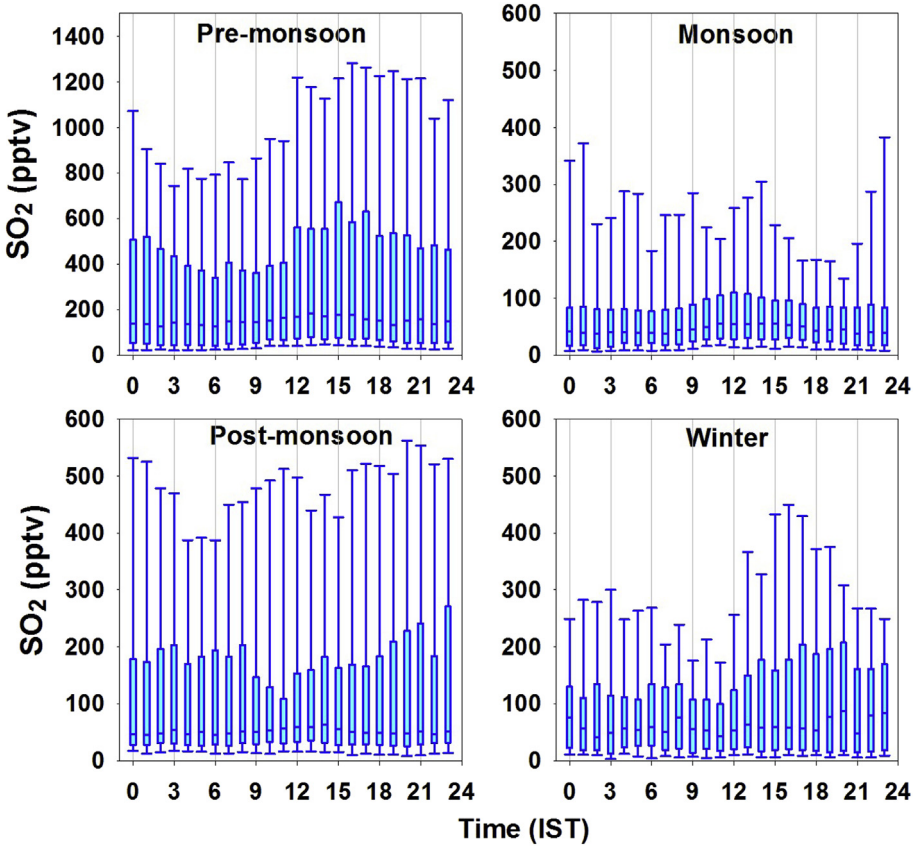

Fig. 2. Diurnal variations in surface SO_2 during four seasons (winter, DJF; pre-monsoon, MAM; monsoon, JJA; post-monsoon SON) at Nainital during 2009–2011.

to 4 ms^{-1} at 1830 IST). Thus, fast advection of air masses from source regions during daytime, elevates SO_2 levels at the study site. The relative humidity (RH) is lowest (32%) during April, thus wet removal processes are supposed to be least influential. RH values start to build up in May (50%) and exceed 90% in July. Oxidative losses of SO_2 during transport from source regions become more probable during these high RH conditions, thus reducing both levels and amplitudes. Wet scavenging of SO_2 by rain and clouds during rainy months (monsoon) brings the levels and amplitudes further down. The levels of SO_2 are lower during winter as influences of emissions could be minimal during this period as the observation site mostly remains above the regional PBL. Moderate correlations ($R^2 = 0.41$) between OMI-PBL SO_2 (which represents regional SO_2) and OMI-free tropospheric SO_2 during winter and post-monsoon corroborate this argument (Fig. 3). However, columnar SO_2 does not seem to have any association with surface concentrations. It is pertinent to mention here that free troposphere refers to a region largely unaffected by the mesoscale planetary boundary layer dynamics. Low levels of SO_2 during winter at Nainital seem to represent background concentrations, though not exactly free tropospheric concentrations, for this region. These concentrations are modulated by cloud processes (in-cloud scavenging). The washout coefficient of SO_2 due to rain is estimated to be about 2.6×10^{-5} s^{-1} times the rate of rainfall (mm/h) (Martin, 1984).

Despite different levels of SO_2 during different months and associated variations in diurnal amplitudes, a common feature in SO_2 diurnal variations over Nainital is the existence of elevated values during daytime (except during January). The first thing that seems responsible for this feature is photochemical oxidation of reduced sulfur compounds during daytime. However, due to very low levels for most of the trace gases (Sarangi et al., 2014), significant contribution of hydrogen sulfide or COS to the SO_2 formation over Nainital seems unlikely. Contributions from DMS also seem unlikely as major natural source of DMS is ocean. Since the role of chemistry appears to be least, the next important factor to cause elevated daytime values in SO_2 could be the impact of vertical winds (w component). Diurnal changes in wind flows play significant role in the diurnal variability of trace gases over the mountains (Kleissl et al., 2007) and it has also been shown for this site (Sarangi et al., 2014). Especially after winter, during pre-monsoon, valley slopes absorb solar radiation and the air adjacent to the valley, now being warm and less dense, starts flowing upslope (valley breeze). The vertical winds start increasing after sunrise and it is upslope (positive) during daytime, which coincides with the observed increase in SO_2 values. At Nainital, the w-wind is maximum during noon hours (about ±0.1 m/s), when SO_2 levels are observed to be the highest. This concurs with the explanation of transport of relatively polluted air from the low altitude areas to the mountain top. The w values show a decreasing tendency towards the evening hours and remain downslope (about −0.1 m/s) during the nighttime due to radiational cooling of valley walls (mountain breeze). This can also result in dilution of SO_2 levels with free tropospheric background air, thus resulting in lower nighttime values. This feature could become very prominent during winter resulting in lowest nighttime values of SO_2 (katabatic type winds). The diurnal variation in w-wind is maximum during pre-monsoon (>0.6 m/s), which corroborates large diurnal amplitude in SO_2. During this time, the w-wind reverses from −0.45 m/s during nighttime to about 0.2 m/s during daytime. During monsoon, the w-wind variation is very low (nighttime: −0.05 m/s and daytime: 0.2 m/s), consequently diurnal amplitude in SO_2 is also very less. Higher SO_2

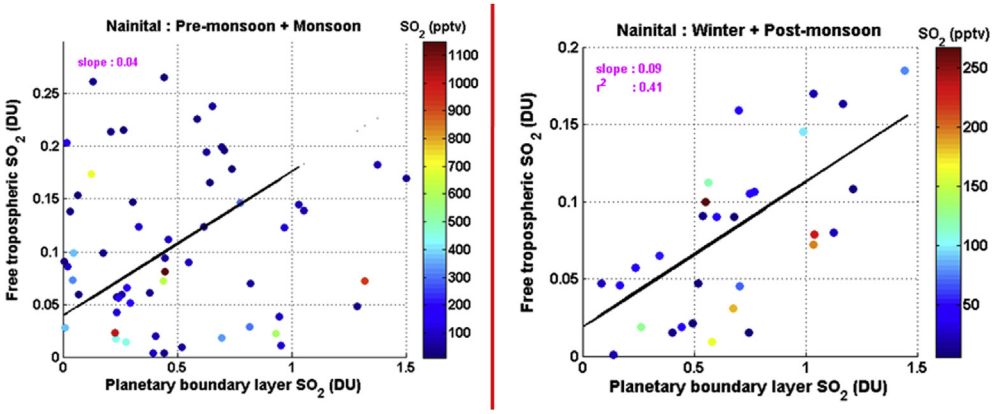

Fig. 3. Variation of PBL and free tropospheric SO_2 from OMI measurements over Nainital. The corresponding measured surface SO_2 mixing ratios are shown in color. (For interpretation of the references to color in this figure legend, the reader is referred to the web version of this article.)

values were also observed in upslope winds by Hanke et al. (2003) during MINATROC field campaign 2000 on Monte Cimone, Italy.

3.2. Seasonal variations in surface SO_2

The monthly SO_2 concentrations over Nainital are shown in Fig. 4. It is observed that SO_2 concentrations are highest during pre-monsoon and lowest during monsoon and winter. In particular, mean SO_2 concentrations above 500 pptv are observed during April. SO_2 concentrations start to build up from February, peak during April and come down during May–June. The SO_2 concentrations are very low during July–August, when this region is under the ambit of monsoon. A slight enhancement in SO_2 levels is observed during September. The observed seasonal variation in SO_2 at Nainital is in sharp contrast to the seasonal SO_2 variations over two megacities in the IGP viz. Delhi (Datta et al., 2011) and Kolkata (Mallik et al., 2014), which show higher mixing ratio during winter.

Observations of SO_2 at other high altitude sites in India are not available and therefore present observations are compared with those available at other global high altitude sites (Table 1). Available data show higher SO_2 values in summer and lower in winter both at Nainital and Sonnblick Observatory in Austria. In case of Sonnblick, a region with Alpine climate, the nearest settlements (Rauris in the North and Heiligenblut, in the South) are well known tourist centers for mountain-related summer and winter activities. Annual average SO_2 at Nainital is more or less similar to values at Mt. Sto. Tomas (Philippines). Annual average values are much lower (lesser than 30 pptv) at three sites (Langtang, Nepal; Mt Kenya, Kenya; Isla Redonda, Argentina) which are above 3500 m. The summer concentrations at Nainital are similar to another nearby high altitude site at on the opposite side of Himalayas (Mt. Waliguan, China). However, the winter concentrations at Nainital are far lower to those at Mt. Waliguan. Over Mt. Fiji in Japan, higher SO_2 is observed during winter despite notable long-range transport during spring. Higher SO_2 during winter at Mt. Fuji is attributed to minimal removal of SO_2 due to cloud processes during winter while the reverse happens during spring (Igarashi et al., 2006).

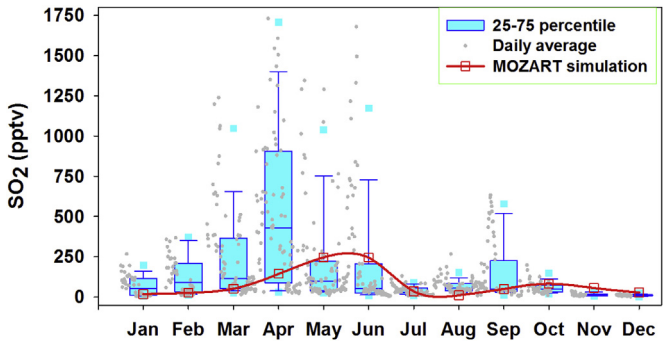

Fig. 4. Monthly variation of surface SO_2 during 2009–2011 at Nainital. Simulations of SO_2 from a global 3D model (MOZART-4) are also shown.

Fig. 4 also shows a comparison between observations and MOZART-4 simulations of the monthly mean SO_2 levels around Nainital. Monthly average values are somewhat comparable with model values lying within the sigma of measured values for most months. Model predicted values are at the lower end of the averaged observed values throughout the year, except during May and June when model values are higher. The model is not able to produce the high peak SO_2 value in April. Influence of changing wind regimes during early spring could be one factor in underestimation of the actual observations in April and this will be discussed in subsequent sections. Observations are made at a high altitude site and we feel that the coarse resolution of the model would not be able to resolve the topography of the region. Nevertheless, several studies show that SO_2 column observed by satellite over polluted regions of East Asia are well reproduced by MOZART (Clarisse et al., 2011).

Seasonal variations of SO_2 can be influenced by seasonal changes in emission strengths, atmospheric circulations and depth of the boundary layer as well as the seasonal strength of removal mechanisms. Seasonal variations in anthropogenic emissions are unlikely to be substantial (Streets et al., 2003) especially for SO_2 where transport (vehicular) and residential sectors play a paltry role against year-long emissions from power plants and industries. Observations at Mt. Fuji also showed that seasonal changes in emissions were not responsible for observed SO_2 changes at its summit (Igarashi et al., 2006).

The transport of SO_2 from source regions in the IGP to Nainital depends highly on the prevalent wind regimes. Wind direction is mainly north-westerly both during pre-monsoon and winter, with the percentage count of this wind-direction being about 20% more in pre-monsoon than in winter. A clinching evidence of the role of transport is demonstrated from good correlations between observed SO_2 concentrations and wind speed (Fig. 5). These correlations are higher during the pre-monsoon and monsoon periods compared to winter, confirming that transport of SO_2 from its emission sources are more effective during the pre-monsoon and

Table 1
Comparison of SO_2 mixing ratios (pptv) over Nainital with measurements at other higher altitude sites.

	Altitude (m)	Summer	Winter	Annual	Period	Referrence
Nainital, India	1958	345 ± 192	71 ± 61	150 ± 155	2009–11	This study
Mt. Waliguan, Tibet	3810	420–490	330–700	410 ± 140	1997–2009	Lin et al. (2013)
Mt. Fuji, Japan	3776		90–130		2002	Igarashi et al. (2004)
Sonnblick Observatory, Austria	3106	260	65		1995–96	Tscherwenka et al. (1998)
Mauna Loa, Hawaii	3400		40–100		1988–89	Luria et al. (1992)
Langtang, Nepal	4676			<30	Sep 1999–00	Carmichael et al. (2003)
Camkoru, Turkey	1350			580	–	–
Mt. Kenya, Kenya	3780			30	–	–
Isla Redonda, Argentina	3459			<30	–	–
Mt. Sto. Tomas, Philippines	2200			110	Sep 1999–00	–
Monte Cimone, Italy	2165	370 ± 535			Jun–July, 2000	Hanke et al. (2003)

monsoon period. Higher wind speeds (mean >3 m/s during March–April) and a deeper boundary layer (daytime mean >2 km) also favor horizontal advection.

Humidity can also play an important role in the variations of SO_2. The monthly average RH during December–February is about 50% while it is lower during March (42%) and April (32%). Higher humidity during winter should favor higher oxidant concentrations and thus greater SO_2 removal (Igarashi et al., 2006; Zhang et al., 2004). Oxidative losses of SO_2 as governed by reaction R1 could impact seasonal distributions. The most dominant oxidation mechanism is by OH, leading to formation of an adduct ($HOSO_2$), which reacts with O_2 to form the sulfuric acid anhydride (SO_3), which further reacts with water to form H_2SO_4, in a rapid, exothermic reaction (−88 kJ mol^{-1}). In the formation of H_2SO_4, R1 is the rate-limiting step.

$$SO_2 + OH + M \rightarrow HOSO_2 + M \quad (R1)$$

$$HOSO_2 + O_2 \rightarrow HO_2 + SO_3 + M \quad (R2)$$

$$SO_3 + H_2O + M \rightarrow H_2SO_4 \quad (R3)$$

The H_2SO_4 formed subsequently condenses, almost irreversibly, on the preexisting particles. It also forms new particles by nucleating with water vapor (H_2O) and gaseous ammonia (NH_3) to form sulfate aerosol. However, the absolute RH values are still very low to account for the humungous seasonal difference in SO_2 concentrations. The characteristic low abundances of OC (range: 2.8–6.9 μg C m^{-3}) and EC (range: 0.34–1.4 μg C m^{-3}) during winter at Manora peak and their significant correlation with K^+ and SO_4^{2-} suggest contribution from long-range transport of anthropogenic species (Rengarajan et al., 2007).

There are other dynamical processes which could also influence SO_2 seasonal variations. It is well known that the variations in the boundary layer heights will have important contribution in determining the levels and diurnal/seasonal variations, in different trace species (Naja and Lal, 2002; Kumar et al., 2010a). During TRACE-P campaign around Yellow Sea, it was observed, that below 2 km SO_2 layers of a few hundred meters depth were often isolated from the mixed layer (Tu et al., 2003). However, since Nainital is a high-altitude site, local boundary layer dynamics affects this region

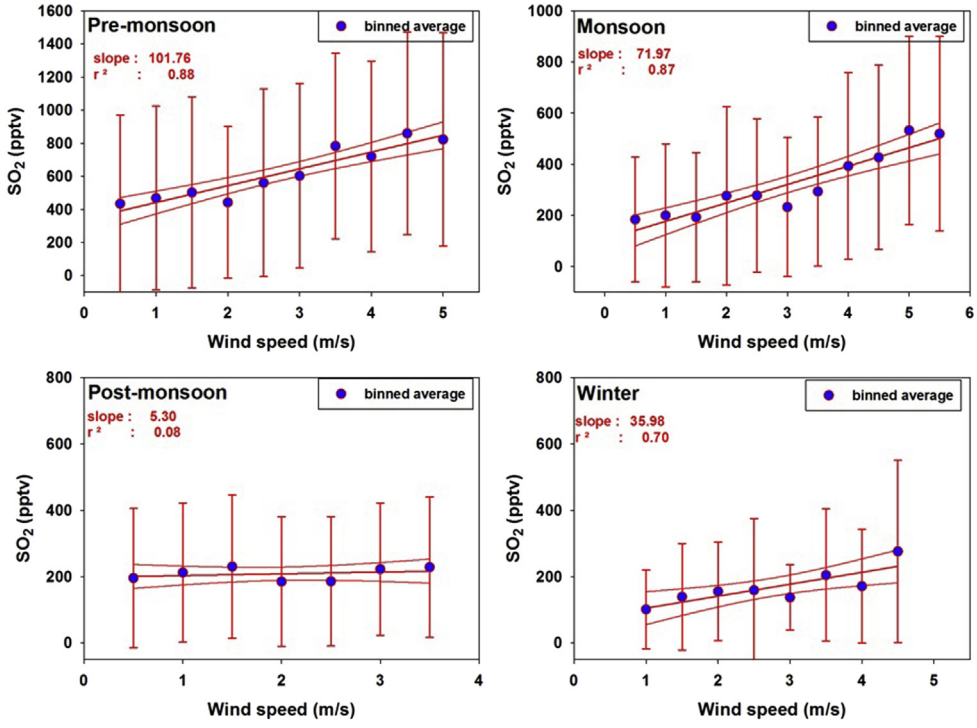

Fig. 5. Variation of surface SO_2 with wind speed at Nainital during four different seasons. The correlations are based on SO_2 averages in 0.5 m/s wind speed bins.

differently as compared to the low lying plains. Fig. 6 shows that strong association exists between SO_2 concentrations and daytime PBL heights. However, during night-time, there is almost no association with PBL heights. This indicates that when the PBL is high, import of SO_2 to the study site is more probable. Extending this argument to seasonal changes in PBL, since PBL is very low during winter, import of SO_2 to the study site is precluded. The average planetary boundary layer height over the region during winter is about 900 m at 1130 IST, 300 m at 1730 IST and below 50 m during nighttime in winter. This implies that the local boundary layer at this site is mostly very low and this region is mostly cut off from the nearby IGP emissions, those are trapped within the regional boundary layer, several meters below the observation site (Sarangi et al., 2014). Thus, despite high SO_2 concentrations in the IGP during winter, boundary layer dynamics acts as a bottleneck in transport of IGP emissions to the study site. This is also corroborated by lower values of carbon monoxide (CO) and nitrogen oxides (NO_y) during winter compared to pre-monsoon (Sarangi et al., 2014).

SO_2 values are lower during monsoon especially during July–August. Since lifetime of SO_2 is about 1.8 days in the boundary layer (Faloona, 2009), therefore long-range transport or even the influence of marine air-mass (south westerly winds) from the Bay of Bengal or Arabian Sea will not play important role. Rather, we feel that wet scavenging might be one of the major causes for lower SO_2 levels in July–August. Nainital receives maximum rainfall in July (mean >600 mm). Thus, efficacy in wet removal processes in determining SO_2 concentrations could be significant during monsoon (Matsuda et al., 2006). The major sinks of SO_2 are oxidation, dry-deposition and wet-deposition, with global average contributions of 53%, 36% and 8% respectively (Faloona, 2009). Rai et al. (2010) have calculated a deposition rate of 185 μg m^{-2} s^{-1} for SO_2 removal at a rainfall rate of 168 mm/h. However, this explanation has to remain qualitative until actual wet deposition over the region is estimated. Further, being a high altitude site, in-cloud scavenging of SO_2 is a very realistic possibility. Such features have been observed at other high altitude sites as well (Igarashi et al., 2004).

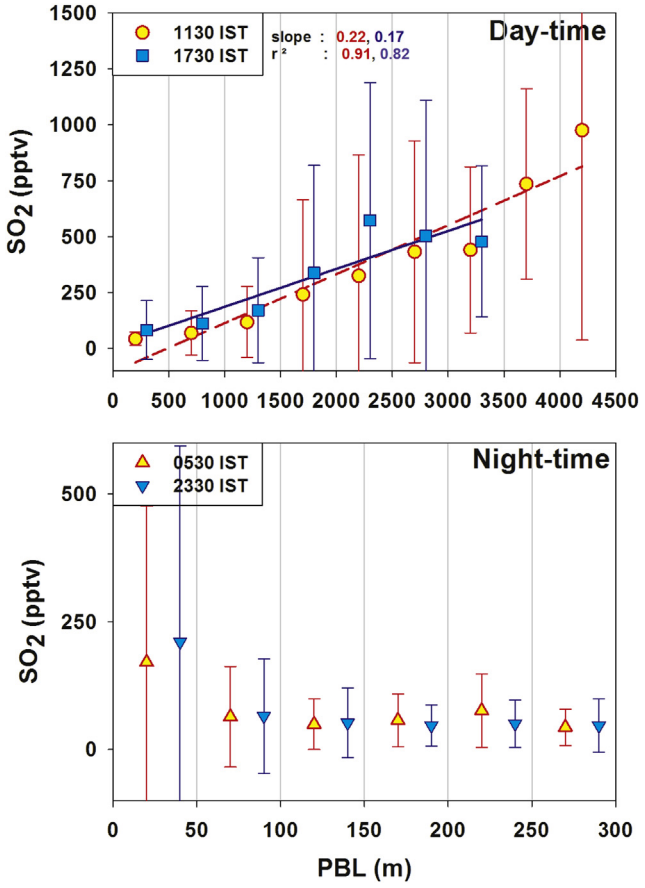

Fig. 6. Variations of surface SO_2 with the planetary boundary layer (PBL) heights over the Nainital region. The correlations are based on SO_2 averages in 500 m PBL bins during daytime and 50 m bins during night-time. PBL height is much lower in night when compared with daytime.

3.3. Probable sources of higher SO_2 during pre-monsoon

The fact that local sources of SO_2 are not likely to be significant at Nainital, accompanied by good correlations of SO_2 with wind speed (Fig. 5) and daytime PBL (Fig. 6) substantiates the role of transport of SO_2 from outside the Nainital region. Since highest SO_2 concentrations are observed during April and May, potential source contribution function (PSCF) analysis (Wang et al., 2009; Mallik et al., 2013b) is done for these months to identify the probable source regions. PSCF is the ratio of polluted trajectory segment endpoints falling in a grid cell to the total number of trajectory endpoints passing over that grid. The PSCF value can be interpreted as the conditional probability that the concentrations of a given pollutant sample greater than the threshold level are related to the passage of air parcels through a grid cell during transport to the receptor site. The analysis suggests that major contributing regions are Northern India (mainly the industrial belt of Punjab-Haryana region) and North-East Pakistan (Punjab and Khyber Pakhtunkhwa) (Fig. 7). The probable source grids falling in Pakistan contain major oil fields and refineries. SO_2 emission factors are higher for oil (0.01–0.08 ton ton^{-1}; highest for fuel oil) compared to coal (0.01 ton ton^{-1}) (Garg et al., 2001). The probable source grids spanning Punjab, Haryana, Northern Rajasthan and Delhi regions of India also contain numerous power plants and have been shown to be major emission sources for SO_2 (Streets et al., 2003; Garg et al., 2001). Delhi, Chandigarh and Rupnagar, located in the northern Indian belt, are among the top 10 SO_2 emitting districts in India. Analysis of SO_2 emissions from Indian districts indicates that the major contributing districts have more than 90% emissions due to coal combustion (Garg et al., 2001). The northern Indian region is also dotted with numerous cement factories and this industry accounts for about 10% of industrial SO_2 emissions in India (Garg et al., 2001).

3.3.1. Satellite based evidence of regional transport

Different analyses in previous sections have shown that the variability in SO_2 levels over Nainital is governed primarily by transport processes and the boundary layer dynamics. Here, an attempt is made to study the variability in data (SO_2, nitrogen dioxide (NO_2) and aerosols index) from space-borne sensors. NO_2 and aerosols index (AI) are also good proxies for anthropogenic emissions. A correlation analysis between surface SO_2 and OMI tropospheric NO_2 shows a positive correlation during monsoon and pre-monsoon (Fig. 8). Fig. 8 also shows a scatter plot between SO_2 and OMI UV Aerosol Index (AI). The AI is insensitive to clouds since large size non-absorbing particles produce near-zero AI values. Over the annual cycle, there is no discernible impact of AI on SO_2 concentrations (or vice versa). However, during pre-monsoon, the daily average SO_2 is well correlated with AI ($R^2 = 0.71$). Similar to AI, good correlations are also observed between daily average SO_2 with OMI absorbing as well as extinction optical depth at both 354 and 500 nm. These correlations are maximum during the month of April ($R = 0.84$ and 0.79 for absorption and extinction respectively). Since both absorption and extinction correlate with SO_2, it is more

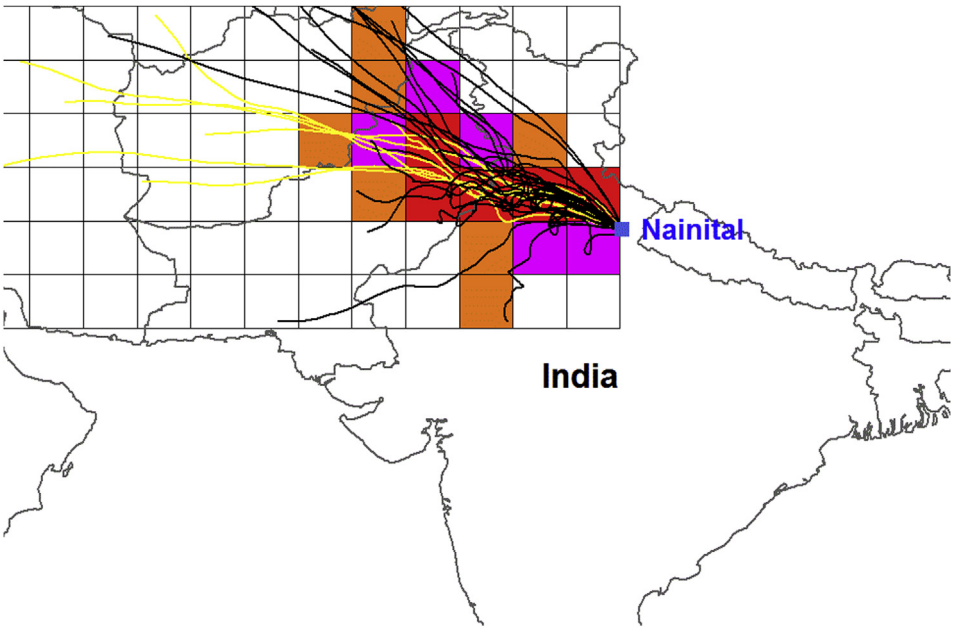

Fig. 7. Probable source regions contributing to elevated SO_2 concentrations over the study location during May. The map is derived from Potential source contribution function analysis using TrajStat software (Wang et al., 2009). Runtime: 72 h, cell size = 2° × 2°. Pollution criteria: 75 percentile of hourly variation of SO_2. The red grids are the most probable source regions, followed by pink and orange. (For interpretation of the references to color in this figure legend, the reader is referred to the web version of this article.)

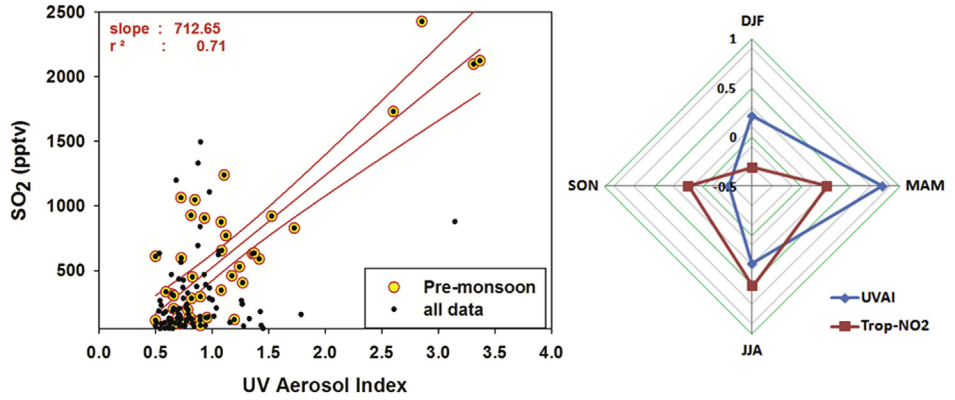

Fig. 8. Co-relation between of daily average SO_2 with UV aerosol index during pre-monsoon. The OMI pass occurs around 1330 IST. Correlations of SO_2 with AI and OMI columnar NO_2 are also shown during four seasons (winter, DJF; pre-monsoon, MAM; monsoon, JJA; post-monsoon SON) in right panel.

likely that the correlations are governed by transport processes rather than transformation processes. It is to be noted that absorbing aerosols (desert dust, smoke) decrease the spectral contrast that yield positive AI value whereas non-absorbing small aerosol particle (sulfate aerosols, weakly absorbing aerosols) results in small negative AI value. Therefore, positive values in AI and strong positive correlation with SO_2 during pre-monsoon indicate that SO_2 is also transported along with dust.

3.3.2. Source signatures from SO_2–NO_y relationships

The relationship between SO_2 and NO_y can serve as a useful indicator to the emission source types. With respect to sources, SO_2 emissions can be broadly classified into power plants and industries, transport sector, residential sector and biomass burning. The residential sector is not a major contributor to SO_2, except in residential areas of cities (Lu et al., 2011), and biomass burning influence, being restricted to certain periods of the year, can be easily identified. In general, a higher SO_2/NO_x ratio (>0.5) indicates

Table 2
$SO_2/NO_{y(x)}$ ratios (same units) at different places. The Olivier et al. references pertain to EDGAR inventory. The Zhang et al. reference pertains to Intex-B inventory.

	SO_2/NO_x	References
Power	1–3	Zhang et al. (2009)
Industry	1–5	–
Transport	<0.1	–
Nainital	0.11–0.57	This study
Turkey	0.27	Tasdemir et al. (2005)
Chinese sites	0.83–1.54	Wang et al. (2004)
USA	0.7	Olivier et al. (1996)
Brazil	0.3	
Australia	0.6	–
Germany	0.9	–
Japan	0.6	–
Korea	1.4	

coal combustion in large point sources (power plants, industries etc) (Parrish et al., 1991). Lower ratios indicate predominance of NO_x and are generally attributed to the transport sector (Aneja et al., 2001). Emission factor for SO_2 due to coal burning in power sector varies between 0.008 and 0.016 Ton Ton^{-1} for the Indian region (Streets et al., 2003). Considering average emissions of 0.8% SO_2 and 1.07% NO_2 from coal burning in power plants, the emission ratio of SO_2/NO_2 in vicinity of power plants should be around 0.9. In India, coal and oil product combustion have almost equal shares in total NO_x emissions. SO_2/NO_x ratios from INTEX-B campaign (Zhang et al., 2009) for different source types are shown in Table 2. For comparison, SO_2/NO_x ratios for different regions of the world adopted from the EDGAR inventory of the year 2000 (Olivier et al., 1996) is also shown.

A SO_2/NO_x ratio of 0.39 ± 0.77 was estimated, based on data from University of Houston's Moody Tower supersite when air masses were arriving from 35 km southwest from a 3800 MW electrical generating unit, the largest of all fossil fuel plants in the U.S. (Luke et al., 2010). SO_2/NO_x ratios for point sources in US were in the range of 0.44–2.3 (Aneja et al., 2001). Wang et al., 2004 have measured a ratio of 1.29 for Linan region of China (representing Chinese anthropogenic emissions) during March 2001. The SO_2/NO_y slope increased from 0.83 during winter nights to 1.26 during non-winter days at Linan, China indicating larger contributions from coal burning (Wang et al., 2002). A SO_2/NO_2 value of 0.12 in the evening hours over Ahmedabad during May, 2010 was attributed to vehicular influences (Mallik et al., 2012). A SO_2/NO_x value of 0.58 for New Delhi was obtained by Aneja et al. (2001) for the period of 1997–98. The SO_2/NO_2 ratios were found to be below 0.2 over several major urban regions of the IGP (Mallik and Lal, 2013). Over Nainital, SO_2 and NO_y seem to correlate well during pre-monsoon but not during winter (Fig. 9). The SO_2/NO_y ratios are higher during this period of convective transport of industrial emissions from IGP with values of 0.57 and 0.40 during pre-monsoon and monsoon. It is possible that NO_y values have decreased during transport, thus increasing the ratio. The SO_2/NO_y ratio will change during transport due to different chemical conversions of SO_2, NO_x and NO_y. Imhoff et al. (2001) have observed increasing SO_2/NO_y ratios in power plant plumes due to faster removal of NO_y. The ratios at Nainital are low during winter (0.11) representing the local background characteristics.

3.3.3. *Influence of fires*

Although emission inventories have pegged the major contribution to SO_2 levels in India to power generation (46%) and industries (36%) (Garg et al., 2001), the share of biomass burning (6%) is not negligible. In general, the SO_2 emission factors for different types of biomass combustions vary between 0.6 and 0.8 g kg^{-1}(Gadi et al., 2003). However, SO_2 emission factors are higher for burning of wood (2.25 g kg^{-1}), agriculture residue and forest biomass (1.55 g kg^{-1}) and animal wastes (1–6 g kg^{-1}), the largest being for dung (Venkataraman et al., 1999). Nevertheless, the northern Indian region has been known to be affected by biomass burning activities during pre-monsoon. These are mainly attributed to farming activities (crop residue burning) with some contribution from forest fires. Since PSCF analysis also shows air masses coming from this region to the observation site during pre-monsoon, it is likely that there could be some contribution from biomass burning activities in elevating the SO_2 levels over Nainital during pre-monsoon.

The impact of the northern Indian biomass burning has been shown to result in the enhancement of ozone levels at Nainital (Kumar et al., 2010b). MODIS monthly fire counts over the northern Indian region (20–38°N, 60–95°E) is significantly higher during April (2700 ± 1500) and maximum during May (4600 ± 1100). The MODIS fire pixel data and SO_2 observations are used to mark the probable source grids. The fire counts are first averaged over larger

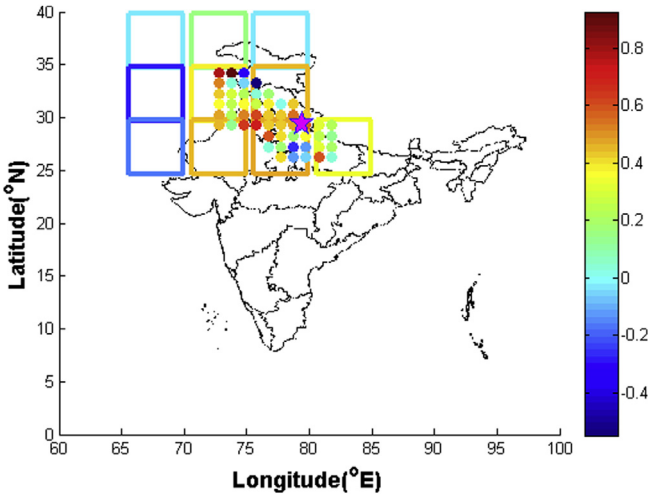

Fig. 10. Correlation of MODIS fire pixel counts over Northern India with SO_2 concentrations measured at Nainital. The boxes represent 5° × 5° grids while the circles represent 1° × 1° grids.

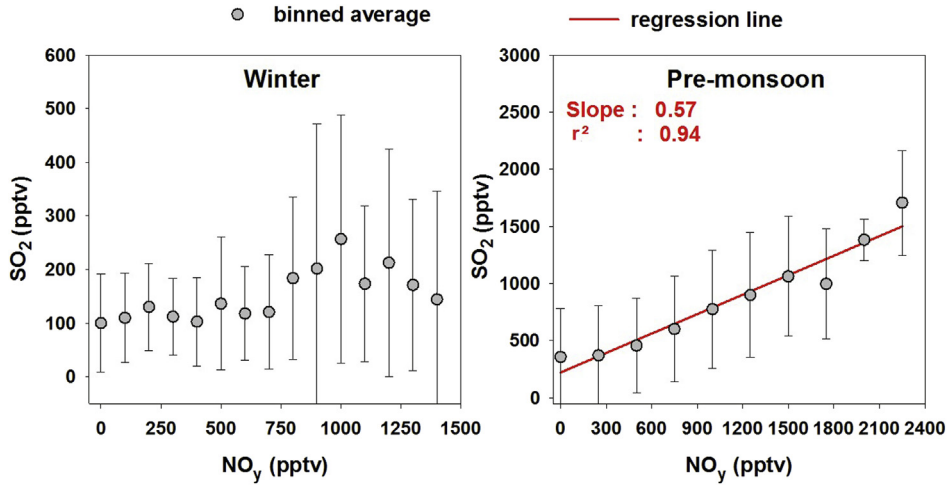

Fig. 9. SO_2–NO_y relationships from measured surface concentrations over Nainital during winter and pre-monsoon.

grids (5° × 5°). Then the temporal changes in fire pixels over these grids are correlated with SO_2 temporal changes over Nainital. Fig. 10 shows that the grids spanning 70–80°E and 25–35°N are positively associated with SO_2 measurements over Nainital during the same period. Interestingly these are the grids where a lot of biomass burning activities occur. Once the large grids are identified, grids of 1° × 1° grids are again identified to again correlate the fire pixel counts over these grids with SO_2 concentrations measured at Nainital. Interestingly, it is observed that the grids that show some association with SO_2 are actually related to biomass burning (Fig. 10). It is to be noted that most of the red and orange dots are in the Punjab-Haryana region, where lot of biomass burning occurs during pre-monsoon.

4. Conclusions

Observations of SO_2 are made at a high altitude site (Nainital) in the central Himalayas during 2009–2011 to have information on emission characteristics of Northern Indian and IGP emissions over this pristine background location. The seasonal variation of SO_2 shows higher values during pre-monsoon and low values (sometimes below the detection limit of the instrument) during winter. The high values during pre-monsoon are attributed to effective transport of air masses (favored by a high PBL) from the IGP and Northern Indian plains to the study location. These regions are dotted with numerous high capacity power plants (thermal, hydro etc) where coal burning occurs. The region also has many cement industries and fertilizer plants, which are major contributors to national SO_2 emissions after power plants and steel industries. The high levels of SO_2 in pre-monsoon are further accentuated during April–May, due to influence of biomass burning in North-Western India. The SO_2 levels come down during monsoon due to oxidation losses, wet scavenging and dilution by monsoon winds. It is also likely that anthropogenic sulfur is preferably transported as sulfate rather than SO_2 during monsoon, when relative humidity increases. Guttikunda et al. (2001) have also estimated high sulfur deposition over the Indian region during summer-monsoon period. Thus, it is important to understand temporal changes in both SO_2 and sulfate concentrations when studying the transport processes. This remains a task for future projects.

The SO_2 levels are very low during winter when the observation site is generally above the regional boundary layer, thereby being cut off from the emissions in the IGP and North-West India. The night-time SO_2 levels during winter are very low, quite often below the detection limit of the instrument, and represent free tropospheric, background concentrations. The diurnal patterns in SO_2 show daytime elevation throughout the year due to convective mixing associated with the boundary layer evolution. The feature is strongest during the noon hours of spring, uplifting the emissions and photo-chemically processed air masses, resulting in largest diurnal amplitudes in SO_2. Strong evidence of transport from IGP is observed from good correlations of SO_2 with wind-speed and NO_y during pre-monsoon. The SO_2–NO_y ratios are higher during pre-monsoon, suggesting influence of emissions from power plants and industries.

MOZART-4 simulations more-or-less agree with SO_2 observations over Nainital for most of the months. The model fails to reproduce the peak concentrations in April, probably because of its coarse resolution. The summertime SO_2 observations over Nainital are very similar to a nearby high-altitude site in Tibet but the winter values over Nainital are by far very low indicating lower background SO_2 over the Indian region. Unlike Mt-Fuji, where summertime SO_2 is low due to wet removal processes, the summertime SO_2 over Nainital compares well with summertime observations at other high altitude sites in Europe. Further, it is observed that SO_2 over Nainital is never enough to breach the air quality standards. Still monitoring of SO_2 over this pristine site must be continued along with initiation of sulfate measurements to have a better understanding of transformation processes in transport plumes. The sulfur species being intrinsically linked to climate, these measurements will provide insight into the sulfur cycle, cloud processes and the climate response to their concentration changes at large, for the Himalayan and South Asian region.

Acknowledgment

We acknowledge the support of Indian Space Research Organization (ISRO-ATCTM Project) and Physical Research Laboratory for this work. We are grateful to the Director of ARIES for providing necessary facilities to make these measurements. We thank technical staff at ARIES for carrying out these measurements. The MOZART model was run on a 3 Terraflop HPC Linux cluster at Physical Research Laboratory.

References

Adhikary, B., Carmichael, G.R., Tang, Y., Leung, L.R., Qian, Y., Schauer, J.J., Stone, E.A., Ramanathan, V., Ramana, M.V., 2007. Characterization of the seasonal cycle of south Asian aerosols: a regional-scale modeling analysis. J. Geophys. Res. 112, D22S22. http://dx.doi.org/10.1029/2006JD008143.

Andreae, M.O., Merlet, P., 2001. Emission of trace gases and aerosols from biomass burning. Glob. Biogeochem. Cycles 15 (4), 955–966.

Aneja, V.P., Agarwal, A., Roelle, P.A., Phillips, S.B., Tong, Q., Watkins, N., Yablonsky, R., 2001. Measurements and analysis of criteria pollutants in New Delhi, India. Environ. Int. 27, 35–42.

Baker, A.K., Schuck, T.J., Brenninkmeijer, C.A.M., Rauthe-Schöch, A., Slemr, F., van Velthoven, P.F.J., Lelieveld, J., 2012. Estimating the contribution of monsoon-related biogenic production to methane emissions from South Asia using CARIBIC observations. Geophys. Res. Lett. 39, L10813.

Biela, B., Moore, R., Benesch, R., Talbert, B., Jacksier, T., 2003. The Do's and Don'ts in the Analysis of Sulfur for Polyolefin Producers. In: Gulf Coast Conference, Galveston Island, TX 2003 paper 81.

Carmichael, G.R., et al., 2003. Measurements of sulfur dioxide, ozone and ammonia concentrations in Asia, Africa, and South America using passive samplers. Atmos. Environ. 37, 1293–1308.

Clarisse, L., Fromm, M., Ngadi, Y., Emmons, L., Clerbaux, C., Hurtmans, D., Coheur, P.F., 2011. Intercontinental transport of anthropogenic sulfur dioxide and other pollutants: an infrared remote sensing case study. Geophys. Res. Lett. 38, L19806. http://dx.doi.org/10.1029/2011GL048976.

Clarisse, L., Clerbaux, C., Dentener, F., Hurtmans, D., Coheur, P.F., 2009. Global ammonia observations derived from infrared satellite observations. Nat. Geosci. 2, 479–483. http://dx.doi.org/10.1038/NGEO55.

Datta, A., Saud, T., Goel, A., Tiwari, S., Sharma, S.K., Saxena, M., Mandal, T.K., 2011. Variation of ambient SO_2 over Delhi. J. Atmos. Chem. http://dx.doi.org/10.1007/s10874-011-9185-2.

Dey, S., Tripathi, S.N., 2008. Aerosol direct radiative effects over Kanpur in the Indo-Gangetic Basin, northern India: Long-term (2001–2005) observations and implications to regional climate. J. Geophys. Res. 113, D04212. http://dx.doi.org/10.1029/2007JD009029.

Emmons, L.K., Walters, S., Hess, P.G., Lamarque, J.-F., Pfister, G.G., Fillmore, D., Granier, C., Guenther, A., Kinnison, D., Laepple, T., Orlando, J., Tie, X., Tyndall, G., Wiedinmyer, C., Baughcum, S.L., Kloster, S., 2010. Description and evaluation of the model for ozone and related chemical tracers, version 4 (MOZART-4). Geosci. Model. Dev. 3, 43–67. http://dx.doi.org/10.5194/gmd-3-43-2010.

Faloona, I., 2009. Sulfur processing in the marine atmospheric boundary layer: a review and critical assessment of modeling uncertainties. Atmos. Environ. 43, 2841–2854.

Fishman, J., Wozniak, A.E., Creilson, J.K., 2003. Global distribution of tropospheric ozone from satellite measurements using the empirically corrected tropospheric ozone residual technique; identification of the regional aspects of air pollution. Atmos. Chem. Phys. 3, 893–907. http://dx.doi.org/10.5194/acp-3-893-2003.

Forster, P., et al., 2007. Changes in atmospheric constituents and in radiative forcing. In: IPCC 2007.

Gadi, R., et al., 2003. Emissions of SO_2 and NO_x from biofuels in India. Tellus 55B, 787–795.

Garg, A., et al., 2001. Subregion (district) and sector level SO_2 and NO_x emissions for India: assessment of inventories and mitigation flexibility. Atmos. Environ. 35, 703–713.

Gautam, R., Hsu, N.C., Lau, K., Tsay, S.C., Kafatos, M., 2009. Enhanced pre-monsoon warming over the Himalayan–Gangetic region from 1979 to 2007. Geophys. Res. Lett. 36, L007704.

Guttikunda, S.K., et al., 2001. Sulfur deposition in Asia: seasonal behavior and contributions from various energy sectors. Water Air Soil Pollut. 131, 336–406.
Hanke, M., et al., 2003. Atmospheric measurements of gas-phase HNO3 and SO_2 using chemical ionization mass spectrometry during the MINATROC field campaign 2000 on Monte Cimone. Atmos. Chem. Phys. 3, 417–436.
Horowitz, L., et al., 2003. A global simulation of tropospheric ozone and related tracers: description and evaluation of MOZART, version 2. J. Geophys. Res. 108, 4784. http://dx.doi.org/10.1029/2002JD002853.
Igarashi, Y., et al., 2006. Seasonal variations in SO_2 plume transport over Japan: observations at the summit of Mt. Fuji from winter to summer. Atmos. Environ. 40, 7018–7033.
Igarashi, Y., Sawa, Y., Yoshioka, K., Matsueda, H., Fujii, K., Dokiya, Y., 2004. Monitoring the SO_2 concentration at the summit of Mt. Fuji and a comparison with other trace gases during winter. J. Geophys. Res. 109, D17304. http://dx.doi.org/10.1029/2003JD004428.
Imhoff, R.E., et al., 2001. NO_y removal from the Cumberland power plant plume. Atmos. Environ. 35, 179–183.
Kar, J., Jones, D.B.A., Drummond, J.R., Attie, J.L., Liu, J., Zou, J., Nichitiu, F., Seymour, M.D., Edwards, D.P., Deeter, M.N., Gille, J.C., Richter, A., 2008. Measurement of low altitude CO over the Indian subcontinent by MOPITT. J. Geophys. Res. 113, D16307. http://dx.doi.org/10.1029/2007JD009362.
Kleissl, J., Honrath, R.E., Dziobak, M.P., Tanner, D., Val Martin, M., Owen, R.C., Helmig, D., 2007. Occurrence of upslope flows at the Pico mountaintop observatory: a case study of orographic flows on a small, volcanic island. J. Geophys. Res. 112, D10S35. http://dx.doi.org/10.1029/2006JD007565.
Krotkov, N.A., Carn, S.A., Krueger, A.J., Bhartia, P.K., Yang, K., 2006. Band residual difference algorithm for retrieval of SO_2 from the Aura Ozone Monitoring Instrument (OMI). Special issue. In: IEEE Trans. Geosci. Rem. Sens., vol. 44(5). AURA, pp. 1259–1266. http://dx.doi.org/10.1109/TGRS.2005.861932.
Kumar, M., Mallik, C., Kumar, A., Mahanti, N.C., Shekh, A.M., 2010a. Evaluation of the boundary layer depth in semi-arid region of India. Dyn. Atmos. Ocean. 49, 96–107.
Kumar, R., Naja, M., Venkataramani, S., Wild, O., 2010b. Variations in surface ozone at Nainital: a high-altitude site in the central Himalayas. J. Geophys. Res. 115, D16302. http://dx.doi.org/10.1029/2009JD013715.
Lal, S., et al., 2012. Light non-methane hydrocarbons at two sites in the Indo-Gangetic Plain. J. Environ. Monit. 14, 1159–1166.
Lawrence, M.G., Lelieveld, J., 2010. Atmospheric pollutant outflow from southern Asia: a review. Atmos. Chem. Phys. 10, 11017–11096. http://dx.doi.org/10.5194/acp-10-11017-2010.
Lin, W.X., Xu, X. Yu, Zhang, X., Huang, J., 2013. Observed levels and trends of gaseous SO_2 and HNO_3 at Mt. Waliguan, China: results from 1997 to 2009. J. Environ. Sci. 25 (4), 726–734.
Luria, M., Boatman, J.F., Harris, J., Ray, J., Straub, T., Chin, J., Gunter, R.L., Herbert, G., Gerlach, T.M., Van Valin, C.C., 1992. Atmospheric sulfur dioxide at Mauna Loa, Hawaii. J. Geophys. Res. 97 (D5), 6011–6012.
Lu, Z., Streets, D.G., Zhang, Q., de Foy, B., Krotkov, N.A., 2013. Ozone monitoring instrument observations of interannual increases in SO_2 emissions from Indian coal-fired power plants during 2005–2012. Environ. Sci. Technol. 47, 13993–14000.
Lu, Z., Zhang, Q., Streets, D.G., 2011. Sulfur dioxide and primary carbonaceous aerosol emissions in China and India, 1996–2010. Atmos. Chem. Phys. 11, 9839–9864.
Luke, W.T., et al., 2010. Measurements of primary trace gases and NO_Y composition in Houston, Texas. Atmos. Environ. 44, 4068–4080.
Mallik, C., Lal, S., 2011. Changing long-term trends in tropospheric temperature over two megacities in the Indo-Gangetic Plain. Curr. Sci. 101 (5), 637–644.
Mallik, C., Venkataramani, S., Lal, S., 2012. Study of a high SO_2 event observed over an urban site in western India. Asia-Pacific. J. Atmos. Sci. 48 (2), 171–180. http://dx.doi.org/10.1007/s13143-012-0017-3.
Mallik, C., Lal, S., Naja, M., Chand, D., Venkataramani, S., Joshi, H., Pant, P., 2013a. Enhanced SO_2 concentrations observed over Northern India: role of long-range transport. Int. J. Rem. Sens. 34 (8), 2749–2762. http://dx.doi.org/10.1080/01431161.2012.750773.
Mallik, C., Lal, S., Venkataramani, S., Naja, M., Ojha, N., 2013b. Variability in ozone and its precursors over the Bay of Bengal during post-monsoon: transport and emission effects. J. Geophys. Res. http://dx.doi.org/10.1002/jgrd.50764.
Mallik, C., Lal, S., 2013. Seasonal characteristics of SO_2, NO_2 and CO emissions in and around the Indo-Gangetic Plain. Environ. Monit. Assess. 186 (2), 1295–1310.
Mallik, C.D., Ghosh, D., Ghosh, Sarkar, U., Lal, S., Venkatramani, S., 2014. Variability of SO_2, CO and light hydrocarbons over a megacity in Eastern India: effects of emissions and transport. Environ. Sci. Poll. Res. 21 (14), 8692–8706.
Martin, A., 1984. Estimated washout coefficients for sulphur dioxide, nitric oxide, nitrogen dioxide and ozone. Atmos. Environ. 18, 1955–1961.
Matsuda, K., et al., 2006. Deposition velocity of O_3 and SO_2 in the dry and wet season above a tropical forest in northern Thailand. Atmos. Environ. 40, 7557–7564.
Mohn, J., Emmenegger, L., 2001. Determination of Sulfur Doixide by Pulsed UV-fluorescence. Swiss Federal Laboritories for Materials Testing & Research.
Naja, M., Lal, S., 2002. Surface ozone and precursor gases at Gadanki (13.5 N, 79.2 E), a tropical rural site in India. J. Geophys. Res. 107 (D14), 4197.
Ohara, T., et al., 2007. An Asian emission inventory of anthropogenic emission sources for the period 1980–2020. Atmos. Chem. Phys. 7, 4419–4444.
Olivier, J.G.J., et al., 2003. Present and Future Surface Emissions of Atmospheric Compounds. POET Rep 2, EU Prof. EVK2-1999-00011. European Union, Brussels.
Olivier, J.G.J., Bouwman, A.F., van der Maas, C.W.M., et al., 1996. Description of EDGAR Version 2. RIVM Report 771060002.
Pant, P., Hegde, P., Dumka, U.C., Sagar, R., Satheesh, S.K., Moorthy, K.K., Saha, A., Srivastava, M.K., 2006. Aerosol characteristics at a high-altitude location in central Himalayas: optical properties and radiative forcing. J. Geophys. Res. 111, D17206. http://dx.doi.org/10.1029/2005JD006768.
Parrish, D.D., Trainer, M., Buhr, M.P., Watkins, B.A., Fehsenfeld, F.C., 1991. Carbon monoxide concentrations and their relation to concentrations of total reactive oxidized nitrogen at two rural U. S. sites. J. Geophys. Res. 96, 9309–9320.
Rai, A., Ghosh, S., Chakraborty, S., 2010. Wet scavenging of SO_2 emissions around India's largest lignite based power plant. Adv. Geosci. 25, 65–70.
Ramachandran, S., Kedia, S., 2012. Radiative effects of aerosols over Indo-Gangetic plain: environmental (urban vs. rural) and seasonal variations. Environ. Sci. Pollut. Res. Int. 19 (6), 2159–2171. http://dx.doi.org/10.1007/s11356-011-0715-x.
Ramanathan, V., Ramana, M.V., 2005. Persistent, widespread, and strongly absorbing haze over the Himalayan foothills and the Indo-Gangetic plains. Pure Appl. Geophys. 162, 1609–1626.
Rengarajan, R., Sarin, M.M., Sudheer, A.K., 2007. Carbonaceous and inorganic species in atmospheric aerosols during wintertime over urban and high-altitude sites in North India. J. Geophys. Res. 112, D21307. http://dx.doi.org/10.1029/2006JD008150.
Sarangi, T., Naja, M., Ojha, N., Kumar, R., Lal, S., Venkataramani, S., Kumar, A., Sagar, R., Chandola, H.C., 2014. First simultaneous measurements of ozone, CO, and NO_y at a high-altitude regional representative site in the central Himalayas. J. Geophys. Res. 119, 1592–1611. http://dx.doi.org/10.1002/2013JD020631.
Sheel, V., Lal, S., Richter, A., Burrows, J.P., 2010. Comparison of satellite observed tropospheric NO_2 over India with model simulations. Atmos. Environ. 44, 3314–3321.
Streets, D.G., et al., 2003. An inventory of gaseous and primary aerosol emissions in Asia in the year 2000. J. Geophys. Res. 108 (D21), 8809. http://dx.doi.org/10.1029/2002JD00309.
Tasdemir, Y.S., Siddik Cindoruk, S., Esen, F., 2005. Monitoring of criteria air pollutants in bursa, Turkey. Environ. Monit. Assess. 110, 227–241.
Tscherwenka, Seiberta, P., Kasper, A., Puxbaum, H., 1998. On-line measurements of sulfur dioxide at the 3 km level over central Europe (Sonnblick observatory, Austria) and statistical trajectory source analysis. Atmos. Environ. 32 (23), 3941–3952.
Tu, F.H., Thornton, D.C., Bandy, A.R., Kim, M.-S., Carmichael, G., Tang, Y., Thornhill, L., Sachse, G., 2003. Dynamics and transport of sulfur dioxide over the Yellow Sea during TRACE-P. J. Geophys. Res. 108 (D20), 8790. http://dx.doi.org/10.1029/2002JD003227.
US Environmental Protection Agency (US EPA), 2002. List of Designated Reference and Equivalent Methods. http://www.epa.gov/ttn/amtic/criteria.html.
Venkataraman, C., Bharadwaj, C., Patwardhan, A., 1999. Anthropogenic sulphate aerosol from India: estimates of burden and direct radioative forcing. Atmos. Environ. 33, 3225–3235.
Wang, T., et al., 2004. Relationships of trace gases and aerosols and the emission characteristics at Lin'an, a rural site in eastern China, during spring 2001. J. Geophys. Res. 109, D19S05. http://dx.doi.org/10.1029/2003JD004119.
Wang, T., Cheung, T.F., Li, Y.S., Yu, X.M., Blake, D.R., 2002. Emission characteristics of CO, NO_x, SO_2 and indications of biomass burning observed at a rural site in eastern China. J. Geophys. Res. 107 (D12), 4157.
Wang, Y.Q., Zhang, X.Y., Draxler, R., 2009. TrajStat: GIS-based software that uses various trajectory statistical analysis methods to identify potential sources from long-term air pollution measurement data. Environ. Model. Softw. 24, 938–939.
Yang, K., Krotkov, N., Krueger, A., Carn, S., Bhartia, P.K., Levelt, P., 2007. Retrieval of large volcanic SO_2 columns from the Aura ozone monitoring instrument (OMI): comparisons and limitations. J. Geophys. Res. 112, D24S43. http://dx.doi.org/10.1029/2007JD008825.
Zhang, M., Uno, I., Yoshida, Y., Xu, Y., Wang, Z., Akimoto, H., Bates, T., Quinn, T., Bandy, A., Blomquist, B., 2004. Transport and transformation of sulfur compounds over East Asia during the TRACE-P and ACE-Asia campaigns. Atmos. Environ. 38, 6947–6959.
Zhang, Q., Streets, D.G., Carmichael, G.R., He, K., Huo, H., Kannari, A., Klimont, Z., Park, I., Reddy, S., Fu, J.S., Chen, D., Duan, L., Lei, Y., Wang, L., Yao, Z., 2009. Asian emissions in 2006 for the NASA INTEX-B mission. Atmos. Chem. Phys. Discuss. 9, 4081–4139.